Russian Physics Journal, Vol. 48, No. 9, 2005

PHYSICS OF SEMICONDUCTORS AND DIELECTRICS

VACUUM ULTRAVIOLET EXCITATION OF RARE-EARTH ION LUMINESCENCE IN STRONTIUM FLUORIDE CRYSTALS

K. V. Ivanovskikh, V. A. Pustovarov, B. V. Shul'gin, and M. Kirm UDC 539.37; 539.12.04

The photoexcitation spectra (70–280 nm) of the Eu^{3+}, Tb^{3+}, Dy^{3+}, Er^{3+}, *and* Tm^{3+} *ion luminescence in strontium fluoride crystals are studied at 8 and 295 K by vacuum ultraviolet spectroscopy using synchrotron-radiation excitation. The processes of transfer of the excitation energy to the impurity centers as well as the relaxation mechanisms of the excited high-energy states of the rare-earth ions are analyzed. The bands corresponding to the interconfiguration 4f–5d transitions and the charge-transfer bands are identified in the photoexcitation luminescence spectra.*

INTRODUCTION

Vacuum ultraviolet (VUV) spectroscopy of rare-earth (RE) ions in wide-gap dielectric crystals, in particular, rare-earth ion luminescence under VUV excitation, is of interest for producing luminescent materials for conversion of VUV-radiation into visible light. These materials can be applied for fabrication of phosphors for mercury-free fluorescent lamps and color laser displays, where a discharge with oscillating electrons (Penning discharge) in rare gases (xenon and neon) is used for VUV excitation [1, 2]. Thus, the investigations in the field of VUV-spectroscopy are aimed at studying the energy-level structure of RE-ions in crystalline matrices and relaxation mechanisms of the excited high-energy states of ions causing luminescence.

In this work, the photoexcitation spectra (PE) of the Eu^{3+} ($4f^6$ electron configuration), $Tb^{3+}(4f^8)$, $Dy^{3+}(4f^9)$, $Er^{3+}(4f^{11})$, and $Tm^{3+}(4f^{12})$ ions in the SrF_2 crystals under excitation by UV and VUV synchrotron radiation are studied.

SAMPLES AND EXPERIMENTAL TECHNIQUE

The strontium fluoride single crystals were grown by K. K. Rivkina and E. G. Morozov at the Pyshmin pilot-production plant of the State Institute of Rare Metals using the Stockbarger method. The fluorides of the RE-elements served as activators. The concentration of the rare-earth ions in synthesized crystals was estimated to be 0.1–1% according to the technique adopted in [3].

The photoexcitation spectra were measured under selective excitation by synchrotron radiation at the SUPERLUMI station of the HASYLAB (DESY, Hamburg) [4]. The samples were placed into a working chamber on a crystal holder of a blowing helium cryostat providing an ultrahigh oil-free vacuum ($<1\cdot10^{-7}$ Pa). The pulses of a synchrotron-radiation storage DORIS were of a Gaussian shape (*FWHM* = 120 ps) and a period of 480 ns. A two-meter vacuum McPeterson monochromator with a resolution of 3.2 Å was used for excitation in the 70–280 nm range. Visible luminescence was recorded with a 0.3 m ARC Spectra Pro-308i monochromator and an R6358P (Hamamatsu) photomultiplier. The luminescence in the VUV-region was recorded with a 0.5 m Pouey-type vacuum monochromator with an instrumental

Ural State Technical University, Ural Polytechnic Institute, e-mail: ikv@dpt.ustu.ru. Translated from Izvestiya Vysshikh Uchebnykh Zavedenii, Fizika, No. 9, pp. 85–89, September, 2005. Original article submitted May 14, 2005; revision submitted June 2, 2005.

 1064-8887/05/4809-0984

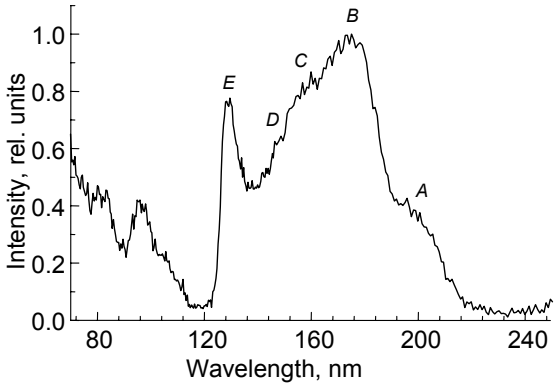

Fig. 1. SrF_2:1% Eu^{3+} crystal, T = 295 K. Photoexcitation spectrum of 590 nm $^5D_0 \rightarrow {}^7F_1$ luminescence in Eu^{3+} ions.

resolution of 10 Å and a solar blind PMT R6836. The PE-spectra were measured at T = 8 and 295 K and normalized to the equal number of photons incident on a sample using sodium salicylate.

RESULTS AND DISCUSSION

The trivalent europium ions ($4f^6$) in wide-gap crystals can be excited due to charge transfer processes and interconfiguration $4f^{n-1}5d \leftrightarrow 4f^n$ transitions [5, 6]. Figure 1 shows photoexcitation spectrum of the 590 nm luminescence in the SrF_2:1% Eu^{3+} crystal transient by the $^5D_0 \rightarrow {}^7F_1$ transitions in the Eu^{3+} ions. The PE-spectrum is largely formed by a wide 138–223 nm non-elementary band that exhibits structure peculiarities at 191–220 nm (denoted by *A*), 173 (*B*), 159 (*C*), and 149 nm (*D*) in Figs. 1–5. As the wavelength of incident photons decreases, one can observe a pronounced band with a maximum at 130 nm (*E*). An effective excitation of the Eu^{3+} ion luminescence is also observed in the vicinity of the long-wavelength edge of fundamental absorption (LWEFA) and in the region of band-to-band transitions (E_g = 11.2 eV (110.7 nm) [7]).

According to [5], the charge-transfer energy between the ligand fluorine and impurity europium ion in fluorites ($F^- \rightarrow Eu^{3+}$) is ~7.8 eV (159 nm), and the threshold of beginning of the spin-allowed interconfiguration $4f^6 \rightarrow 4f^5 5d$-transitions is ~8.4 eV (148 nm). Thus, the major part of the 138 – 223 nm band appears to be formed due to the processes of charge transfer $F^- \rightarrow Eu^{3+}$ and spin-allowed interconfiguration transitions to the lowest levels of the $4f^5 5d$-configuration. The low-energy part of the 138–223 nm band, in particular, the *A* region is, probably, due to the processes of charge transfer involving oxygen ions $O^{2-} \rightarrow Eu^{3+}$, which are uncontrollably present in a crystal. The intense *E*-band may be attributable to the interconfiguration transition to the second component of splitting of the $4f^6 5d$-configuration of the Eu^{3+} ion by the crystal field [6]. No peculiarities related to transitions to higher components of splitting of the $4f^6 5d$-configuration are observed, which is evidently due to intensive matrix absorption.

The Tb^{3+}, Dy^{3+}, Er^{3+}, and Tm^{3+} ions are related to the group of heavy lanthanoids (the number of *f*-electrons > 7), for which both spin-allowed and spin-forbidden interconfiguration $4f^{n-1}5d \leftrightarrow 4f^n$ transitions are possible. The transitions between the levels of the $4f^n$-configuration and the high-spin ion state *HS* of the $4f^{n-1}5d$-configuration are parity-forbidden. The transitions involving the low-spin state *LS* are spin-allowed. The peculiarities of formation of the PE-spectra of heavy rare-earth ions are considered in detail in [8 – 10].

Figure 2 shows a PE-spectrum of luminescence in a SrF_2:0.1% Tb^{3+} crystal caused by the $^5D_3 \rightarrow {}^7F_6$ transitions in the Tb^{3+} ions. The most intense excitation band (*A*) is observed at 211 nm and corresponds to the transition to the lowest low-spin state *LS* of the $4f^7 5d$-configuration and to the beginning of spin-allowed interconfiguration transitions. A phonon-free line is prominent at 213.5 nm (A_1) in the structure of this band. As the wavelengths of incident photons decrease, intensive excitation of luminescence is manifested in the spectral bands at 192 (*B*), 184 (*C*), 178 (*D*), and 174 nm (*E*) as well as in the wide non-elementary bands at 142–166 nm (*F*) and 120–138 nm (*G*). The latter has a fine structure.

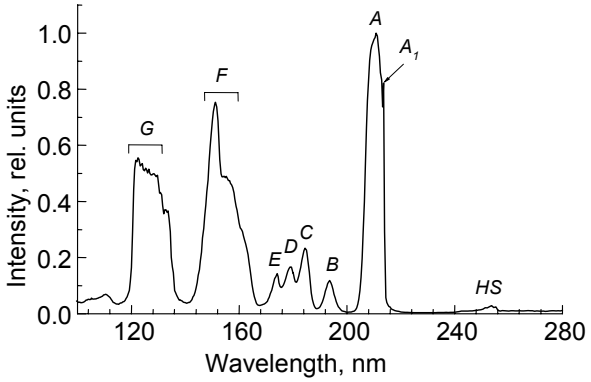

Fig. 2

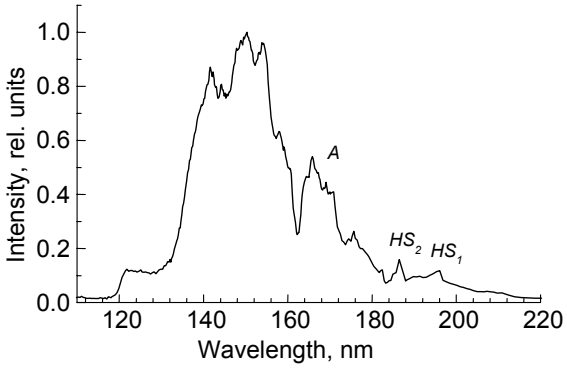

Fig. 3

Fig. 2. SrF_2:0.1% Tb^{3+} crystal, T = 8 K. Photoexcitation spectrum of 380 nm $^5D_3 \rightarrow {}^7F_6$ luminescence in Tb^{3+} ions.

Fig. 3. SrF_2:0.1% Dy^{3+} crystal, T = 8 K. Photoexcitation spectrum of 480 nm $^4F_{9/2} \rightarrow {}^6H_{15/2}$ luminescence in Dy^{3+} ions.

The crystalline field and spin-orbital interaction split the 5*d*-states of a shell. Due to characteristic features [9], the *A* and *G* bands, having a fine structure, correspond to the transitions to the lowest 5*d*-levels ^2E. The transitions to the high-energy splitting components $^2T_2$ are represented in the PE-spectrum by the *C* and *F* bands, the latter including three components. The *B*, *D*, and *E* bands can be caused by the interaction of a *5d*-electron with a 4*f*-electron continuum. The characteristic of the PE-spectrum near 255 nm (Fig. 2) is related to spin-allowed transitions to the lowest high-spin state *HS* of the $4f^7 5d$-configuration.

In the regions, where the band-to-band transitions in SrF_2 begin and separate electron-hole pairs are generated, the excitation intensity of the Tb^{3+} ions does not exceed 10% of that in the maximum of the spectrum. (Hereinafter, the region of band-to-band transitions is not shown in figures).

Figure 3 shows the photoexcitation spectrum of the 480 nm luminescence in the SrF_2:0.1% Dy^{3+} crystal caused by the intraconfiguration $^4F_{9/2} \rightarrow {}^6H_{15/2}$ transitions in the Dy^{3+} ions. Luminescence is excited in the transmission band of the crystal and is represented by a number of bands in the 118 – 212 nm region of the PE-spectrum. A sharp increase in the PE-spectrum intensity near 171 nm (*A*) corresponds to the beginning of the $4f^9 \rightarrow 4f^8 5d$ spin-allowed transitions. As the wavelengths of incident photons decreases, a structure of the excited levels of the $4f^8 5d$-configuration is observed. The complexity of the spectrum is due to additional bands caused by the strong interaction of the 5*d*-electron with the 4*f*-electron continuum and to a great number of vibronic bands [8].

If the energy difference between the two lowest high-spin states is less than that between the lowest low-spin and high-spin states, two spin-forbidden transitions can be observed in the PE-spectra [10]. In our case, such a situation manifests itself by the two low intense characteristics at 196 and 186 nm denoted as HS_1 and HS_2 in Fig. 3. In addition, the high-energy $4f^9 \rightarrow 4f^9$ transitions can contribute to the PE-spectrum formation in the neighborhood of these features [10, 11].

Under excitation in the LWEFA region and in the region of generation of the separate electron-hole pairs, the impurity-center luminescence is suppressed indicating that the efficiency of the energy transfer with the participation of excitons is low.

In addition to visible luminescence caused by the intraconfiguration $4f^n \rightarrow 4f^n$ transitions, the Er^{3+} and Tm^{3+} ions show luminescence in the VUV-region caused by the radiative interconfiguration $4f^{n-1}5d \leftrightarrow 4f^n$-transitions [10]. The excitation processes of the *f–f*- and *d–f*-luminescence of the Er^{3+} and Tm^{3+} ions in SrF_2 have a number of characteristic features discussed below.

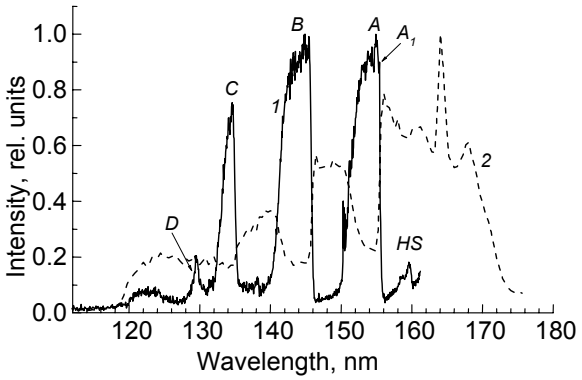

Fig. 4

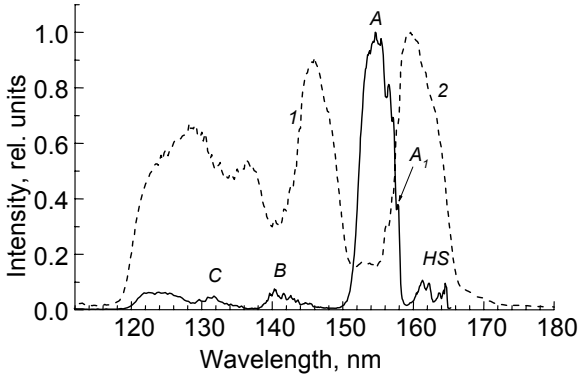

Fig. 5

Fig. 4. SrF_2:1% Er^{3+} crystal, T = 8 K. Photoexcitation spectrum of 165 nm $4f^{10}5d(HS) \rightarrow 4f^{11}(^4I_{15/2})$ luminescence (*1*) and 550 nm $^4S_{3/2} \rightarrow {}^4I_{15/2}$ luminescence in Er^{3+} ions.

Fig. 5. SrF_2:1% Tm^{3+} crystal, T = 8 K. Photoexcitation spectrum of 166 nm $4f^{11}5d$(HS) $\rightarrow 4f^{12}(^3H_6)$ luminescence (*1*) and 451 nm $^1G_4 \rightarrow {}^3H_6$ luminescence in Tm^{3+} ions.

Figure 4 shows the PE-spectra of the *f–f*- and *d–f*-luminescence of the Er^{3+} ions in the SrF_2:1% Er^{3+} crystals. The 164 nm luminescence caused by the spin-forbidden $4f^{10}5d(HS) \rightarrow 4f^{11}(^4I_{15/2})$ transition in the Er^{3+} ions has the highest intensity under excitation near 154 (*A*), 144 (*B*), 134 (*C*), and 130 nm (*D*) (Fig. 4, *1*). These bands are associated with transitions to the ^2E-levels of the $4f^{10}5d$-configuration and have a fine structure. The most intense band *A* includes a weak phonon-free band 155.4 nm (A_1) and corresponds to the transition to the lowest low-spin state *LS* of the $4f^{10}5d$-configuration and to the beginning of the spin-allowed $4f^{11} \rightarrow 4f^{10}5d$-transitions. The transitions caused by filling the high-energy $^2T_2$ states are not observed in the PE-spectrum of the *d–f*-luminescence. A low intense 159 nm band corresponds to the spin-forbidden $4f^{11} \rightarrow 4f^{10}5d(HS)$-transition and the beginning of excitation of the *d–f*-luminescence of the Er^{3+} -ions.

The PE-spectrum of the 550 nm luminescence in the SrF_2:1% Er^{3+} crystals ($^4S_{3/2} \rightarrow {}^4I_{15/2}$ transitions in the Er^{3+} ions) is antibatic to the PE-spectrum of the *d–f*-luminescence. The presence of an intense broad non-elementary 156 – 173 nm band in the PE-spectrum of the *f–f*-luminescence is indicative of the fact that effective excitation of the *f–f*-luminescence is observed at energies lower than the excitation threshold of the radiative interconfiguration transitions. This band has a complex structure, where a narrow intense band at 164 nm is clearly pronounced. The band corresponds (according to its position) to the $4f^{10}5d(HS) \rightarrow 4f^{11}(^4I_{15/2})$ luminescence. As the wavelengths of incident photons decrease, broad bands at 145–154 and 134–143 nm are observed in the PE-spectrum. The antibatic behavior of the *f–f*- and *d–f*-luminescence spectra is atypical for Er^{3+} ions in other matrices (see, for example, [12]).

The PE-spectra of the *d–f*- and *f–f*-luminescence of the Tm^{3+}ions in the SrF_2:0,3% Tm^{3+} crystals have similar properties (Fig. 5). The low-energy excitation threshold of the 167 nm *d–f*-luminescence caused by the $4f^{11}5d(HS) \rightarrow 4f^{12}(^3H_6)$ transitions in the Tm^{3+} ions is manifested in the PE-spectrum by a singularity near 163 nm and corresponds to the spin-forbidden $4f^{12} \rightarrow 4f^{11}5d(HS)$ transition (Fig. 5). With a decrease in the photoexcitation wavelength, a drastic increase in the spectrum intensity is observed, which manifests itself as a structure band at 155 nm (*A*) including a weak phonon-free band at 157.8 nm (A_1). This band corresponds to the beginning of the spin-allowed $4f^{12} \rightarrow 4f^{11}5d$-transitions in the Tm^{3+} ions. As the wavelengths of incident photons decrease, the low intense structure peculiarities are observed at 141 (*B*) and 132 nm (*C*). These are caused by the transitions to the second and third orders of the ^2E-states of the $4f^{11}5d$-configuration. No transitions to the high-energy $^2T_2$ levels are observed in the spectrum.

The PE-spectrum of the 451 nm *f–f*-luminescence of the Tm^{3+} ions ($^1G_4 \rightarrow {}^3H_6$ transitions) in the SrF_2:0,3% Tm^{3+} crystals is antibatic with respect to the PE-spectrum of the *d–f*-luminescence. This spectrum has the highest maxima at 156–165, 141–150, and 119–138 nm. The latter band has an additional special feature at 134–139 nm.

Thus, a common property of the excitation processes of the Er^{3+} and Tm^{3+} ions is a pronounced competition between the intracenter relaxation processes of the high-energy (VUV) Er^{3+} and Tm^{3+} ion excitations to the radiative levels of ions of the $4f^{n-1}5d$- and $4f^n$-configurations. As a result, the PE spectra of the *d–f*- and *f–f*-luminescence of these ions are antibatic.

This phenomenon is likely to be due to a strong electron-dipole interaction between the excited levels of the $4f^{n-1}5d$-configuration and the electron continuum of the 4*f*-shell of the Ln^{3+} ion in the SrF_2 crystal. For the same reason, additional bands appear, and the PE-spectra of the Ln^{3+} ions in the VUV-region become more complicated.

The *d–f*-luminescence intensity of the Er^{3+} and Tm^{3+} ions significantly decreases under excitation of the SrF_2 crystal in the LWEFA region. At the same time, the excitation efficiency of the *f–f*-luminescence remains sufficiently high. On further decrease in the wavelengths of incident photons down to 60 nm, all components of the impurity luminescence of the SrF_2:1% Er^{3+} and SrF_2:0.3% Tm^{3+} crystals are suppressed. Thus, the energy-transfer processes from the matrix to the Ln^{3+} ions by an electron-hole mechanism are ineffective.

The autoionization process beginning with formation of a Ln^{4+} ion may be one of the reasons for the fact that the *f–f*-luminescence in the LWEFA region is excited more effectively than the *d–f*-luminescence. Further capture of a free electron can be described by the model of an exciton localized at the impurity center $Ln^{4+}+e^-$. The relaxation of the autoionized state occurs primarily by energy transfer to the levels of the $4f^n$-configuration through a dipole-dipole interaction [5].

CONCLUSION

The photoexcitation spectra of luminescence of the SrF_2:Ln^{3+} (Ln^{3+} = Eu^{3+}, Tb^{3+}, Dy^{3+}, Er^{3+}, Tm^{3+}) crystals are investigated at T = 8 and 295 K using the VUV-spectroscopy.

High-energy (VUV) excitations of the Eu^{3+} ions cause both the interconfiguration $4f^6 \rightarrow 4f^5 5d$-transitions and charge-transfer processes $F^- \rightarrow Eu^{3+}$. The bands associated with the spin-allowed and spin-forbidden $4f^n \rightarrow 4f^{n-1}5d$-transitions are found in the PE-spectra of luminescence from the ions of the second half of the lanthanide series. The results obtained show that the energy differences between the lowest low-spin *LS* and high-spin *HS* levels of the $4f^{n-1}5d$-configuration are ~7620 cm^{-1}, ~7460 cm^{-1}, ~1750, and ~1600 cm^{-1} for Tb^{3+}, Dy^{3+}, Er^{3+}, and Tm^{3+} ions, respectively, which is in good agreement with the data obtained for these ions in other crystals [8]. The processes of excitation of luminescence from the Er^{3+} and Tm^{3+} ions in the SrF_2 crystal have a similar character. The competition between the excitation processes of the *f–f*- and *d–f*-luminescence manifesting itself in the antibatness of the PE-spectra in the range of the incident-photon energies close to the positions of levels of the $4f^{n-1}5d$-configuration is a unique phenomenon never observed for these ions in other matrices. The competition between the intracenter relaxation processes of high-energy excitations as well as the complication of the PE-spectra observed in a number of cases are caused by the strong interaction between the 5*d*-electron and 4*f*-continuum of the Ln^{3+} ions in the SrF_2 crystal.

For all objects investigated, the luminescence of the Ln^{3+} ions is most pronounced under intracenter excitation. The energy-transfer processes involving intrinsic electron excitations proved to be effective only for europium ions.

The authors are sincerely grateful to V. N. Makhov (Lebedev Physical Institute of RAS) for useful discussions of the work.

The present work was supported in part by the Russian Foundation for Basic Research (Grant 05-02-16530), by the Program “Russian Universities” (Grant UR.02.01.433), by REC-005 (EK-005-XI), and BMBF (05KS8GMD/1).

REFERENCES

1. C. R. Ronda, T. Justel, and H. Nikol, J. Alloys and Comp., **225**, 534–538 (1995).
2. V. N. Makhov, J. Y. Gesland, N. M. Khaidukov, *et al.*, Proc. Fifth Int. Conf. on Inorg. Scintillators and Their Applications, Moscow (1999).
3. A. P. Zyryanov, K. K. Rivkina, B. V. Shul’gin, *et al.*, Izv. AN SSSR Neorg. Mater., **7**, No. 5, 968–969 (1972).
4. G. Zimmerer, Nucl. Instr. and Meth. A, **308**, No. 1–2, 178–186 (1991).

5. A. N. Belsky and J. C. Krupa, Displays., **19**, 185–196 (1999).
6. L. Van Pieterson, M. F. Reid, M. F. Wegh, *et al*., Phys. Rev. B, **65**, 045113 (16) (2002).
7. L. K. Ermakov, P. A. Rodnyi, and N. V. Starostin, Fiz. Tverd. Tela, **33**, No. 9, 2542–2545 (1991).
8. L. Van Pieterson, M. F. Reid, G. W. Burdick, and A. Meijerink, Phys. Rev. B, **65**, 045114 (13) (2002).
9. L. Van Pieterson, M. F. Reid, and A. Meijerink, Phys. Rev. Lett., **88**, No. 6, 067405 (2002).
10. R. T. Wegh and A. Meijerink, Phys. Rev. B, **60**, 10820–10830 (1999).
11. R. T. Wegh, A. Meijerink, R.–J. Lamminmäki, and J. Hölsä, J. Lumin., **87–89,** 1002–1004 **(**2000).
12. V. N. Makhov, N. M. Khaidukov, N. Yu. Kirikova, *et al*., Nucl. Instr. and Meth. A, **470**, 290–294 (2001).